

# Design of an Electrochemical Impedance Test Cell with Servomechanically Adjustable Cell Constant

Hongshen Ma (Student Member), Jeffrey H. Lang (Fellow), and Alexander H. Slocum (Member)

Massachusetts Institute of Technology  
Cambridge, MA, USA  
hongma@mit.edu

**Abstract**— This paper presents the design of an electrochemical impedance test cell for which the cell constant can be precisely varied so as to enable accurate, calibration-free measurements of the dielectric constant and conductivity of liquids and gases. This impedance test cell uses spherical electrodes separated by an adjustable small gap ranging from less than 1  $\mu\text{m}$  up to 50  $\mu\text{m}$ . Accurate material property measurements can be obtained by leveraging the dimensional accuracy of the spheres and the mechanical accuracy of the positioning mechanism. The accuracy of this impedance cell has been demonstrated in measurements of the dielectric constant of air and methanol.

## I. INTRODUCTION

Accurate measurement of the dielectric constant and conductivity of liquids and gases is an important chemical analysis technique with a wide range of applications such as controlling boiler water quality in power plants [1], optimizing the performance of battery electrolytes [2], and detecting chemical products in microfluidic analysis systems [3]. The apparatus used to make these measurements is known as an impedance test cell. A key problem in improving the accuracy of dielectric constant and conductivity measurements is the design of an impedance test cell that enables accurate extraction of the intrinsic parameters of dielectric constant and conductivity from the measurable quantities of capacitance and resistance. The relationship between these quantities are described by,

$$C = \varepsilon / K_{cell} + C_0 \quad (1)$$

$$G = \kappa / K_{cell} + G_0 \quad (2)$$

where  $C$  and  $R$  are the measured capacitance and resistance;  $\varepsilon$  and  $\kappa$  are the dielectric constant and conductivity;  $K_{cell}$  is a geometrical conversion factor known as the cell constant; and  $C_0$  and  $G_0$  are the stray capacitance and conductance. Accurate evaluation of  $K_{cell}$  can be difficult for practical electrode geometries because of the natural uncertainties associated with the stray signals,  $C_0$ , and  $G_0$ . Furthermore, the value of  $K_{cell}$  can also be affected by manufacturing errors, as well as interfacial effects at the electrode-electrolyte boundary.

Existing conductivity sensors typically address the uncertainty of  $K_{cell}$  by periodically calibrating the impedance test cell using standard solutions with known values of  $\varepsilon$  and  $\kappa$ . This correction is of limited value since  $C_0$ , and  $G_0$  can also be dependent on  $\varepsilon$  and  $\kappa$ . As a result, this correction is useful only when the calibration and sample liquids have similar values of  $\varepsilon$  and  $\kappa$  [2, 4].

One method to improve the accuracy of dielectric constant and conductivity measurements, and enable the development of a calibration-free technique, is to design an impedance test cell where  $K_{cell}$  can be varied in a predictable manner. The values of  $\varepsilon$  and  $\kappa$  can be determined from the differential values of  $C$  and  $G$  while the corresponding variations of  $C_0$  and  $G_0$  are kept within a specified accuracy threshold. The fundamental tradeoff in the design of such mechanisms is to maximize the range of  $K_{cell}$  to improve the estimates of  $\varepsilon$  and  $\kappa$ , while minimizing the variation to  $C_0$  and  $G_0$ .

Adjustment of the cell constant can typically be accomplished by either varying the area where the sample and the applied electrical field intersect [2], or by adjusting the electrode separation [5]. This paper studies the possibility of creating an adjustable impedance test cell where the electrodes are at a small distance apart, from tens of microns to less than one micron. Scaling down the electrode separation has the advantage of enlarging the range over which  $K_{cell}$  can be varied while minimizing the errors caused by variations of  $C_0$  and  $G_0$ .

Small, adjustable electrode gaps between planar electrodes can be difficult to design since the effect of parallelism errors between the electrodes becomes greatly magnified at small gaps. This problem can be eliminated using spherical electrodes, where the closest points between two spheres are intrinsically tangent to one another. Spherical shapes are simple to manufacture and can be produced with extremely accurate diameters. Furthermore, spheres can also be produced with nanometer smooth surfaces, reducing the minimum electrode gap and thereby improving the ability to vary  $K_{cell}$ .

---

This work has been supported by MIT's Center for Bits and Atoms under NSF Grant #CCR-0122419.

## II. THEORY

The capacitance between two closely spaced spherical electrodes has the expression [6]

$$C = \pi r \epsilon_r \epsilon_0 \log\left(\frac{2r}{\xi}\right) + C_0, \quad (3)$$

where  $\xi$  is the distance between the spheres at their nearest points,  $r$  is the radius of the spheres,  $\epsilon_0$  is the vacuum permittivity,  $\epsilon_r$  is the relative dielectric constant, and  $C_0$  is a constant. This expression has the property that the spatial derivative of  $C$  is inverse-linear with  $\xi$  such that

$$\frac{dC}{d\xi} = -\frac{\pi r \epsilon_r \epsilon_0}{\xi}. \quad (4)$$

Therefore the dielectric constant can be determined by a series of measurements of  $dC/d\xi$  and  $\xi$ . Owing to the derivative nature of this measurement, the values of  $\xi$  can be replaced by  $\xi = x - x_0$ , where  $x$  is the coordinate measured along the axis in which the sphere is displaced and  $x_0$  is a constant offset. With further manipulation, (4) becomes

$$-\pi r \epsilon_0 \left(\frac{dx}{dC}\right) = \frac{x - x_0}{\epsilon_r}. \quad (5)$$

The value of the relative dielectric constant,  $\epsilon_r$ , can then be determined by fitting (5) to the linear equation

$$y = a + bx \quad (6)$$

where  $\epsilon_r = 1/b$ .

From a discrete set of values for  $C_n$  and  $x_n$ , the derivative  $dx/dC$  can be estimated using the secant approximation

$$\frac{dC}{dx} = \frac{C_{n+1} - C_n}{x_{n+1} - x_n} \quad (7)$$

where  $dC/dx$  is evaluated at  $x = (x_{n+1} + x_n) / 2$ .

The analysis for determining conductivity is exactly analogous to the analysis for determining dielectric constant, where capacitance is replaced by conductance and dielectric constant is replaced by conductivity such that

$$-\pi r \left(\frac{dx}{dG}\right) = \frac{x - x_0}{\kappa}. \quad (8)$$

## III. DESIGN

### A. Electrode

The spherical electrodes are fabricated using a silicon-nitride sphere as a substrate for a thin platinum electrode film. The silicon-nitride spheres have a diameter of 9.52564 mm with a tolerance of  $\pm 0.00013$  mm (Cerbec Saint Gobain Ceramics: Grade 3 spheres). The spheres have a measured (Zygo profilometer) Ra surface roughness of 2 nm with a peak-to-valley range of approximately 50 nm. These values are comparable to polished silicon wafers, which have

a surface roughness Ra of 1 nm and a peak-to-valley range of 20 nm. The electrode film consists of a 50 nm platinum layer and a 5 nm chromium adhesion layer. The metal films are deposited on one hemisphere of the silicon-nitride spheres using electron-beam deposition.

Given the surface roughness of the electrodes, a reasonable minimum electrode gap is 1  $\mu\text{m}$ . Therefore, based on electrode gaps from 1  $\mu\text{m}$  and 50  $\mu\text{m}$ , the cell constant, determined from (3), varies from 7.30  $\text{m}^{-1}$  to 12.7  $\text{m}^{-1}$ .

### B. Electrode Mounting Shaft

The electrode mounting shaft is designed to provide mechanical constraint for the electrodes and to make electrical contact with the platinum film. The electrode mount consists of a 12.7 mm diameter cylindrical shaft where one end has been bored out for the electrode sphere. A ring nut holds the electrode sphere inside the bore with only a small region protruding as shown in Fig. 1. Two dimples on the ring nut allow it to be tightened using a special wrench. When tightened, the ring nut bends slightly and applies a mechanical preload to the electrode to ensure that the electrode and shaft are tightly bound together. Mechanical contact between the ring nut and the electrode also serves as the electrical contact between the platinum film and the mounting shaft. Therefore, the mounting shaft becomes part of the electrode for measuring impedance.

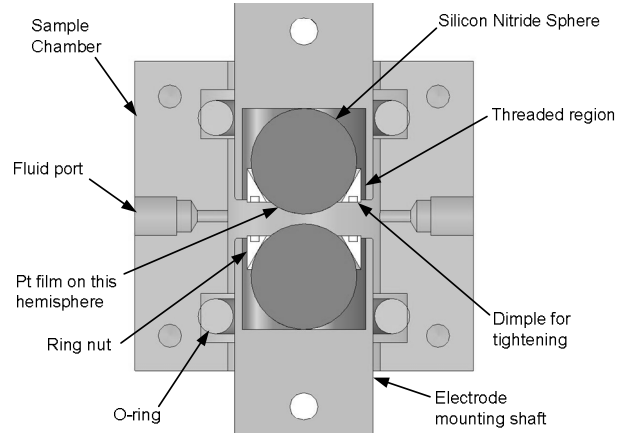


Figure 1. Cross section of the impedance test cell

The capacitance and conductance between the two mounting shafts is the primary contributor of parasitic capacitance and conductance. Based on a simple parallel-plate capacitance model, the stray signal from this source is expected to contribute up to 30% of the measured signal for  $C$ . However, since the separation between the mounting shafts is significantly greater than the separation between the spheres, variation of the stray signal is considerably smaller. Detailed analysis show that the error in the measured dielectric constant caused by this signal is not expected to exceed 0.7% over the range of the cell constant modulation.

The electrode separation is modulated by precise adjustment of the position of the mounting shaft using a

flexural stage. Both mounting shafts are along an aligned axis along the flexure mechanism, and are electrically isolated via a 50  $\mu\text{m}$  layer of polyimide film (McMaster: 2271K72). The position of each mounting shaft along its axial direction is measured using a commercial capacitance probe (Lion precision) as shown in Fig. 2. The measurement of the  $x$ -coordinate is therefore the sum of the two capacitance probes. In order to prevent the capacitance probe from interfering with the impedance measurement, grounded target electrodes are epoxied to the outer edge of each shaft.

### C. Sample Chamber

The sample chamber is designed to constrain the sample fluid between the electrodes while allowing small modulations of the electrode separation. As shown in Fig. 1, the sample chamber consists of a stainless steel cube with dimensions of 27.9 mm x 30.5 mm x 25.4 mm. The mounting shafts slide through a central bore of 13.7 mm. A liquid seal is established between each mounting shaft and the sample chamber via a Kalrez o-ring (#206 Dupont compound 4079), which offers similar solvent resistance to Teflon, but with significantly greater flexibility.

It is important to note that when the electrode separation is adjusted over the limited range of 50  $\mu\text{m}$ , the o-ring does not slip against the shaft of the sample chamber. Rather, the o-rings act as flexures that facilitate this deflection by bending. Unlike a sliding contact that suffers from hysteric errors caused by the sliding friction between the two surfaces, deflection by bending is mechanically repeatable.

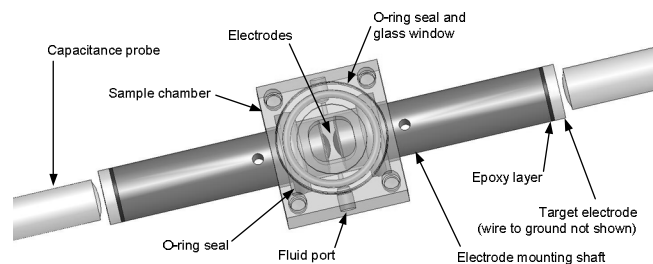


Figure 2. Impedance test cell with capacitance probes and target electrodes

Liquid samples are introduced into the sample chamber via fluidic ports for 1/16-inch OD tubing (Upchurch: M-644-03), connected to a standard syringe. The inlet port is located near the bottom of the chamber while the outlet port is located near the top in order to prevent air bubbles from accumulating in the chamber. The chamber also contains a window for debugging purposes. This window is covered with a 3mm thick round Pyrex window (Esco products: P705125) and is sealed by another Kalrez o-ring.

### D. Mechanism for Adjusting the Cell Constant

The relative position of the electrode mounting shaft is controlled by a monolithic positioning mechanism shown in Fig. 3. Functionally, this mechanism consists of a coarse

adjustor, a fine adjustor, and a metrology frame. The coarse adjustor is a manual lead screw that displaces the bottom mounting shaft. Assuming this screw can be adjusted in  $1^\circ$  increments, the resolution of the coarse adjustor is 0.9  $\mu\text{m}$ .

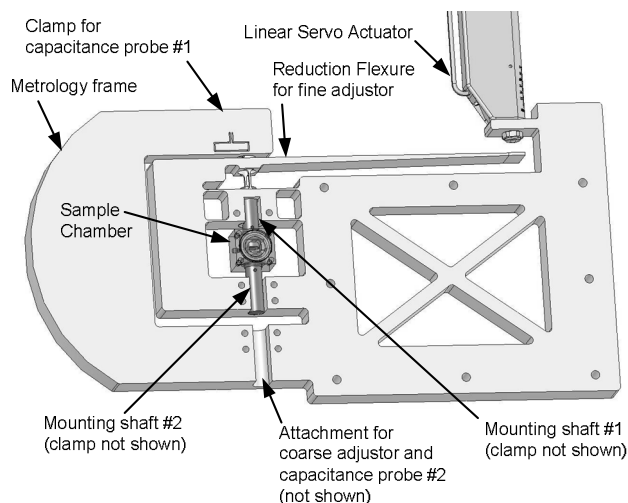


Figure 3. Mechanism for adjusting electrode separation

The fine adjustor consists of a linear servo actuator and a flexural transmission. The actuator is a servo motor and lead screw assembly with 50 nm resolution (Newport: LTA-HL). The flexural transmission is a cantilever flexure that reduces the travel of the actuator by a factor of 190:1, thereby improving the actuator resolution from 50 nm to 0.25 nm. The overall range of the fine adjustor is 50  $\mu\text{m}$ . The fine adjustor design is also optimized to minimize error motion along axes perpendicular to the measurement axis. Analysis by a simple geometric model indicates the effect of these errors is orders of magnitude below the errors caused by fringing fields.

The electrode mounting shafts are clamped to the adjustment mechanism between two half cylinders surfaces. During installation, the top shaft is rigidly clamped first while the bottom shaft is adjusted by the coarse actuator. After the desired coarse position has been reached, the bottom shaft is then clamped and further adjustment of the electrode spacing is accomplished through the fine adjustor.

The metrology frame is designed to constrain the capacitance probes for measuring the position of the electrode mounting shafts. As shown in Fig. 3, the bottom capacitance probe uses the same attachment with the coarse adjustor. Therefore, this probe is designed to be added only after completing the coarse adjustment.

### E. Impedance Measurement

The sample impedance is measured using an Agilent 8424A LCR meter. The measurements are made at 120 kHz, above the frequency where interfacial phenomena begins to affect the measurement.

#### IV. RESULTS

The utility of this impedance test cell has been demonstrated in dielectric constant measurements involving air and methanol. Fig. 4 shows the data from air where the  $x$ -axis is the position of the electrode measured by the capacitance probes; the  $y$ -axis is  $-\pi\epsilon_0\Delta x/\Delta C$  as derived in (5); and the relative dielectric constant is the inverse of the slope. Since the differential value of  $C$  is greater when the electrodes are closer together, the data from smaller electrode gaps is less noisy than the data from larger electrode gaps. The variable level of uncertainty is addressed using an appropriate weight function that gives more weight to the data points from smaller electrode gaps. Using the weighted least squares (WLS) fit, the dielectric constant of air within 1% of the known value of 1.00 has been obtained.

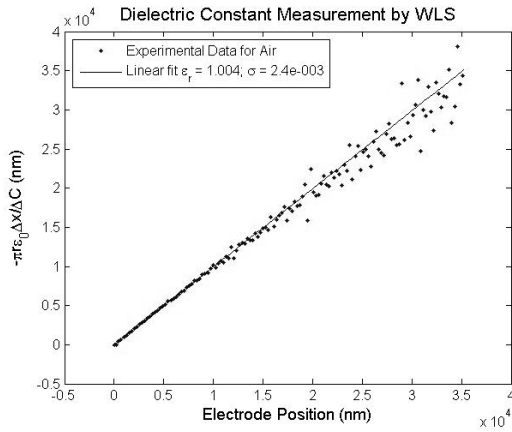


Figure 4. Measurement of the  $\epsilon_r$  of air by WLS fitting

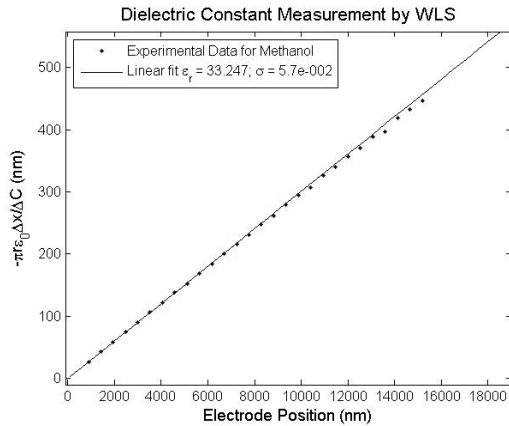


Figure 5. Measurement of the  $\epsilon_r$  of methanol at 21.6°C by WLS fitting

Fig. 5 shows the measurement of the dielectric constant of methanol at 21.6°C. This data show considerably less noise than the air data because of the larger capacitance signal. Fig. 6 shows the results from 20 repeated measurements of the  $\epsilon_r$  for methanol. The results fall well within a  $\pm 1\%$  range of the known value of 33.26 for this temperature. Furthermore, the estimated standard deviation,

$\sigma$ , from one measurement of  $\epsilon_r$  correlates well with the  $\sigma$  determined from repeated measurements.

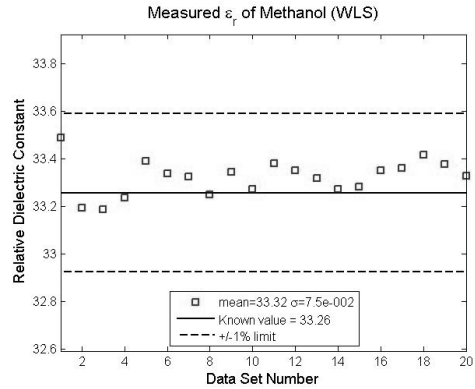


Figure 6. Repeated measurements of the  $\epsilon_r$  of methanol at 21.6°C

#### V. CONCLUSIONS

An impedance test cell with adjustable cell constant for measuring the dielectric constant and conductivity of liquids and gases has been designed and tested. The test cell uses spherical electrodes with adjustable separation from 1  $\mu\text{m}$  to 50  $\mu\text{m}$ . Adjustment of a small electrode gap maximizes the variation of the parasitic capacitance and conductance to enable accurate material property measurements without calibration. Measurements of the dielectric constant of air and methanol confirm the capability of this device to make calibration-free measurements with better than 1% accuracy.

#### ACKNOWLEDGMENTS

H.M. would like to thank Kurt Broderick and Mark Belanger for their help with the fabrication of this device.

#### REFERENCES

- [1] Y. C. Wu, W. F. Koch, and K. W. Pratt, "Low Electrolytic Conductivity Standards," *Journal of the Research of the National Institute of Standards and Technology*, vol. 100, pp. 191-201, 1991.
- [2] S. L. Shiefelbein, N. A. Fried, K. G. Rhoads, and D. R. Sadoway, "A High-Accuracy Calibration-Free Technique for Measuring the Electrical Conductivity of Liquids," *Review of Scientific Instruments*, vol. 69, 1998.
- [3] T. G. Drummond, M. G. Hill, and J. K. Barton, "Electrochemical DNA sensors," *Nature Biotechnology*, vol. 21, pp. 1192-1199, Oct 2003.
- [4] J. P. Wu and J. P. W. Stark, "A high accuracy technique to measure the electrical conductivity of liquids using small test samples," *Journal of Applied Physics*, vol. 101, Mar 2007.
- [5] J. P. Wu and J. P. W. Stark, "A low-cost approach for measuring electrical conductivity and relative permittivity of liquids by triangular waveform voltage at low frequencies," *Measurement Science & Technology*, vol. 16, pp. 1234-1240, May 2005.
- [6] L. Boyer, F. Houze, A. Tonck, J. L. Loubet, and J. M. Georges, "The Influence of Surface-Roughness on the Capacitance between a Sphere and a Plane," *Journal of Physics D-Applied Physics*, vol. 27, pp. 1504-1508, Jul 14 1994.